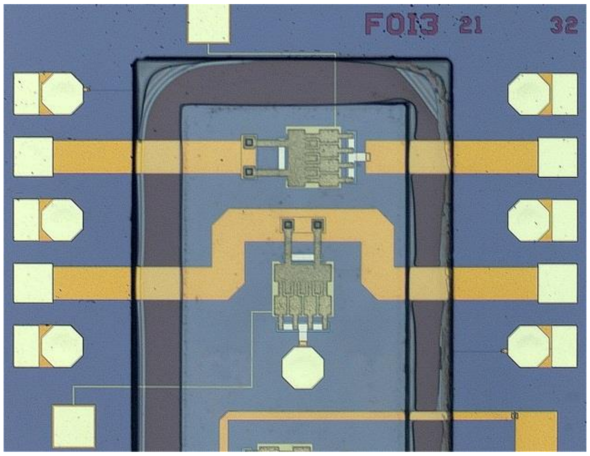

Figure 1. Micrograph of wafer-level packaged GaAs MMIC micro-strip based (series and shunt) RF-MEMS switches.

Figs. 2a-b show measured and simulated up-state and down-state transmission (s_{21}) of some BCB capped series and shunt GaAs MMIC RF-MEMS switch circuits, respectively. The 0-level packaged micro-strip GaAs MEMS switches were characterized at 5-40 GHz using a probe station, an Agilent N5245A PNA-X network analyzer and on-wafer calibration standards (to exclude the effects of the RF pads). The measured and simulated results which are found to be in an over-all agreement up to Ka-band validate the wafer-level packaged GaAs MEMS SPST switch performance. The BCB cap used for protection of the MEMS switches during wafer dicing was not included in the simulations and the results show that the BCB cap has only a marginal effect on the switch performance at these frequencies. The measured ON state (down-state) s_{21} of the 0-level packaged GaAs MEMS series switch is below 0.5 dB up to 24 GHz (s_{21} is equal to 0.5 dB also at 40 GHz) whereas the measured OFF state (up-state) s_{21} corresponds to better than 20 dB of isolation up to 25 GHz. Fig. 2a also shows some resonances in the measured s_{21} data at 34-35 GHz which can be explained by undesired coupling from the nearby (i.e. too closely spaced) shunt switch structure (see Fig. 1) and these effects were taken into account in the circuit simulations.

Fig. 2b shows that the 0-level packaged GaAs MEMS shunt switch has 0.1-0.5 dB of measured transmission losses at 5-40 GHz and isolation is higher than 10 dB up to 12 GHz. Since such GaAs MEMS switches show very low losses and higher isolation at lower frequencies up to X-band/Ku-band they could be potential candidates for use in wideband power limiter circuits. Such GaAs MMIC RF-MEMS switching (and also power limiting) devices could be integrated on the same chip as the active RF circuitry (e.g. with low-noise amplifiers or even in complete receiver front-ends) [2-4]. To test the RF power survivability of some GaAs MEMS shunt switches the input power level P_{in} (at 18 GHz) was increased up to 37 dBm (5 W) when some switch failures were found to occur. Self-actuation tests made on such MEMS shunt switches showed a power limiting effect of 11 dB when P_{in}=27-36 dBm (V_{bias} was reduced below the nominal switch voltage).

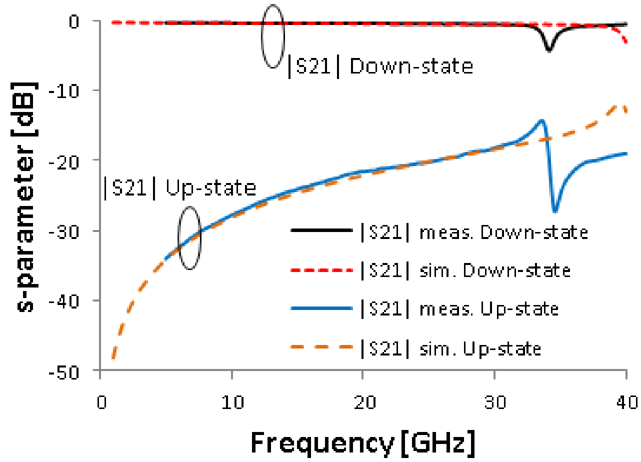

a)

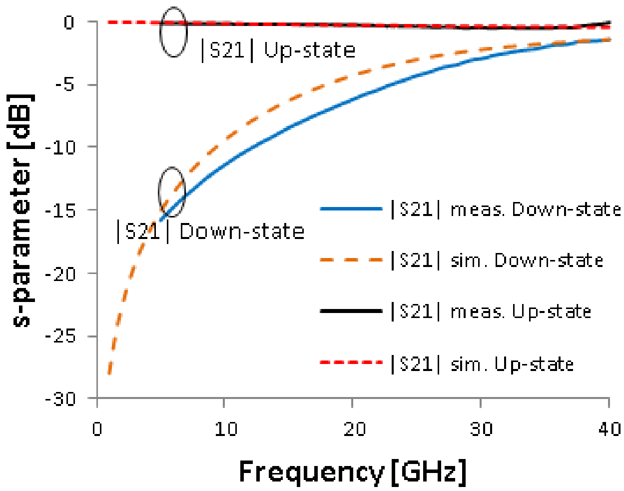

b)

Figure 2. Measured and simulated s_{21} (up-state/down-state) of two 0-level packaged GaAs MMIC RF-MEMS (SPST) switches: a) series and b) shunt.

B. Ka-Band RF-MEMS GaAs MMIC Phase Shifter and LTCC based Phased Array Antenna Modules

The validated GaAs MEMS switch has been used in the design and fabrication of reconfigurable MMIC building blocks such as low-loss switching and phase shifting circuits for various applications up to the mm-wave range. Fig. 3 shows a chip photo of a Ka-band 3-bit MEMS phase shifter circuit that was fabricated within the same GaAs MMIC process run at OMMIC (chip dimensions equal 2x3 mm^2). The three bits that are realized using switched delay lines were designed to give a combined maximum relative phase shift of 315° at 35 GHz (i.e. 45°, 90° and 180° of relative phase shifts, respectively). A certain phase shift is introduced when the two MEMS switches situated in the shorter (reference) path are in the down-state position (V_{bias}>$V_{actuation}$) and the other two switches within the longer (delay) path and are in the up-state position (i.e. biased with 0 V). A relative phase shift is realized when both the switches within the reference part as well as the two switches within the delay path are down.

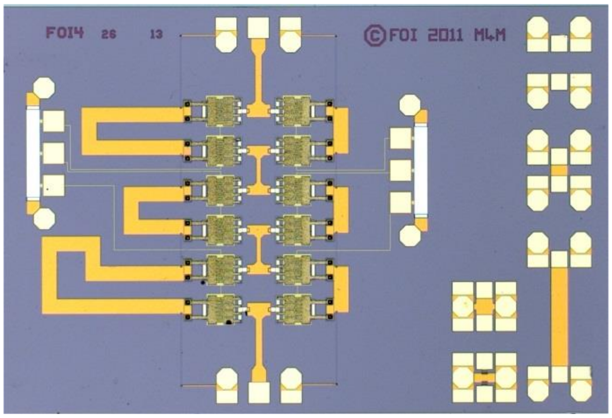

Figure 3. Micrograph of a Ka-band 3-bit RF MEMS phase shifter fabricated using a GaAs MMIC foundry process (the active circuit area used is 4 mm^2).

Fig. 4a-c show experimental results of the 3-bit MEMS phase shifter MMIC for the 000, 001, 010, 100, 111 states (i.e. corresponding to 45°, 90°, 180° and 315° of expected relative phase shifts at 35 GHz, respectively). The measured combined relative phase shift (i.e. for the 111 state) is equal to 315° and 350° at 32 GHz and 35 GHz, respectively (the 001, 010 and 100 states result in roughly 50-60°, 100-110° and 170-190° of relative phase shifts at those frequencies). Fig. 4b shows that the measured input and output matching (s_{11} and s_{22}) is better than -10 dB and -8 dB from 5 GHz up to 34 GHz and 35 GHz, respectively, for all measured states. The measured minimum and maximum transmission losses equal 4.1 dB and 5.7 dB at 32 GHz (i.e. in the reference 000 state and the maximum delay 111 state, respectively). The measured average loss is 4.9 dB at 32 GHz. A proposed Figure-of-Merit (FoM) [7] defined as the relative phase shift ($\Delta\phi$) divided with the average losses ($|s_{21}|$) and the phase shifter circuit area gives that the presented 3-bit GaAs MEMS phase shifter circuit has an FoM=16°/dB·mm^2 at 32 GHz. The state-of-the-art 35 GHz GaAs 3-bit RF-MEMS phase shifter presented in [8] achieved a lower average loss (2dB) but also occupied a somewhat larger chip area of 9 mm^2 (FoM=16°/dB·mm^2).

Figs. 5a-b show photographs of two Ka-band phased array antenna modules made on LTCC that use 1:2 and 1:4 feed networks, respectively. The phase shifter modules (that were fabricated using an LTCC process at VTT) are intended to be populated with some 0-level packaged GaAs RF-MEMS 3-bit phase shifter circuits that have not been characterised so far (same design as shown in Fig. 3). Fig. 6 shows the measured and simulated s_{11} of two LTCC series fed patch antenna elements (i.e. a single row) and which are found to be in a close agreement up to 34 GHz (the measured s_{11} equals -7 dB at 35 GHz which is 10 dB lower than simulated). The measured maximum antenna gain is estimated at 7 dB. Fig. 7 shows the measured s-parameter data of a 1:2 feed network made on LTCC. The measured s_{21} is between -3.3 to -3.8 dB at 20-35 GHz (corresponding to 0.3-0.8 dB of RF losses) while s_{11} and s_{22} are below -10 dB from 22 GHz to 36 GHz.

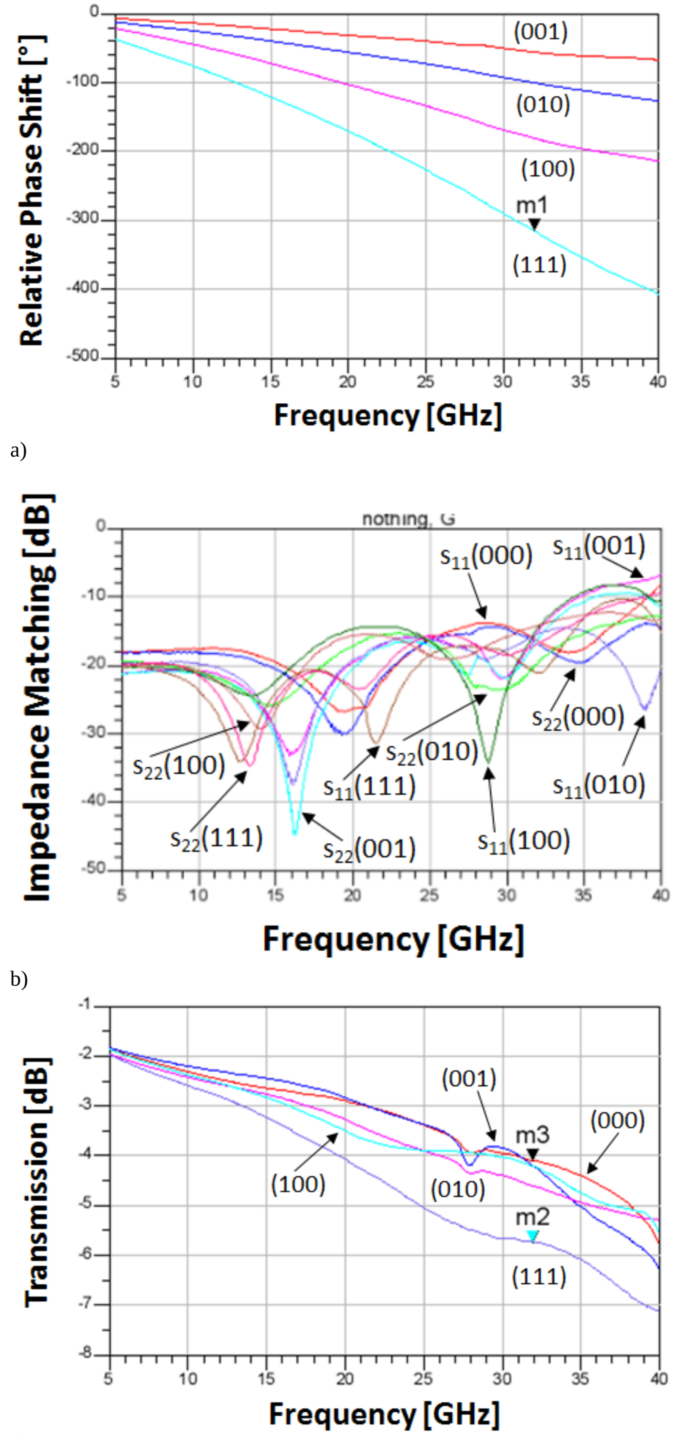

Figure 4. Measured results of a 3-bit RF-MEMS phase shifter circuit fabricated using a GaAs MMIC foundry process: a) relative phase shift and b-c) input/output matching (s_{11}/s_{22}) and transmission losses (s_{21}) for the 000, 001, 010, 100 and 111 states, respectively.

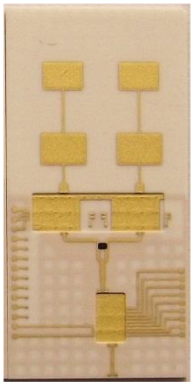
a)

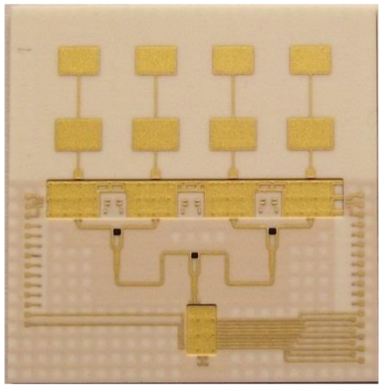
b)

Figure 5. Micrographs of two Ka-band phased array antenna modules made on LTCC (before assembly of RF-MEMS based MMIC 3-bit phase shifters) and using a) 1:2 and b) 1:4 feed networks, respectively.

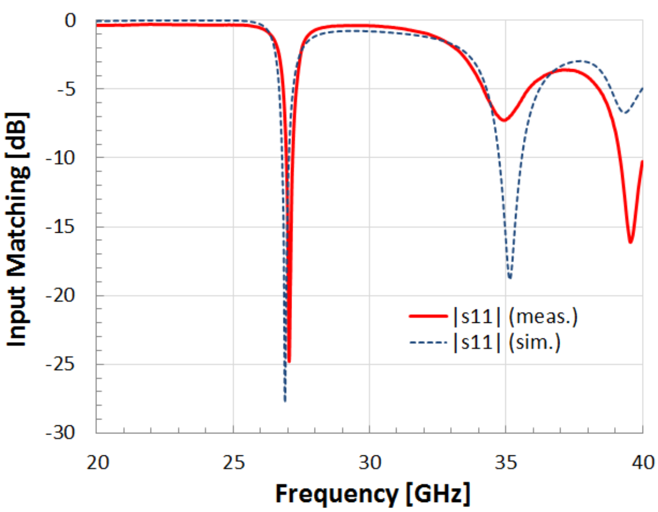

Figure 6. Measured and simulated input matching (s_{11}) of two 35 GHz series fed patch antenna elements (a single row) fabricated on LTCC.

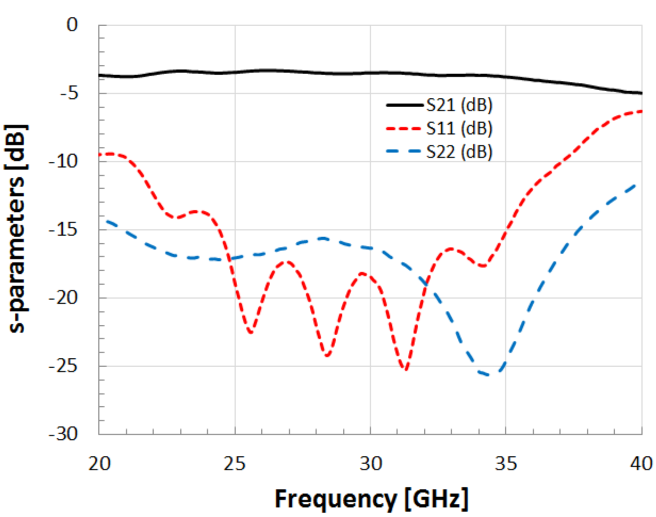

Figure 7. Measured s-parameters of a Ka-band (1 to 2) feed network made on LTCC.

C. *V-BAND/W-Band GaAs RF-MEMS Switching Circuits and On-Chip Antenna*

Relatively few results have been reported related to GaAs MMIC based RF-MEMS switching circuits at frequencies above Ka-band. A Co-Planar Waveguide (CPW) based GaAs MEMS SPST series switch with less than 1 dB of losses up to 95 GHz (together with >15 dB of isolation up to 40 GHz) was presented in [9]. However, those GaAs MEMS switch circuits were made without any on-chip active RF circuitry. Fig. 8 shows a photograph of some RF-MEMS SPST and V-band (Dicke) switch circuits (to the left and right, respectively) that have been fabricated on 200 µm GaAs wafers using OMMIC's 70 nm mHEMT process technology and without including any backside processing (i.e. without the possibility of including any via holes used in micro-strip circuit designs). All circuits included on the 70 nm GaAs RF-MEMS run were made as co-planar designs (which can increase somewhat the circuit dimensions needed) but on the other hand the somewhat risky back-side processing step (as we are considering here the fabrication of unprotected RF-MEMS switches) could be avoided at this stage. A primary goal here was to be able to experimentally validate the expected RF performance when combining on the same wafer for the first time high-frequency low-noise 70 nm mHEMT transistors with some low-loss RF-MEMS switch circuits for mm-wave applications up to W-band.

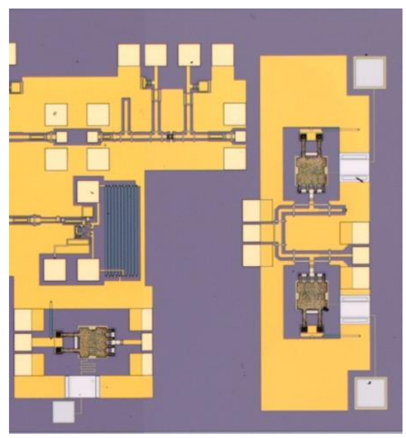

Figure 8. Micrograph of some RF MEMS based SPST and V-band Dicke switch circuits fabricated using a GaAs MMIC foundry process.

Figs. 9a-b show measured and simulated s-parameter data of a CPW GaAs RF-MEMS series switch (shown in Fig. 8). The ON and OFF state transmission/isolation and impedance matching (s_{21} and s_{11}) were obtained from two-port measurements with the GaAs MEMS series switch actuated (in the down-state) and also without any applied DC bias voltage (in the up-state). The 2-110 GHz measurement data shown in Figs.9a-b were obtained after on-wafer calibration at the RF probe tips using a standard calibration substrate (the results include then also RF losses in the RF pads). The measured OFF state isolation is in a relatively close agreement with simulations up to 110 GHz ($s_{21} \leq -10$ dB up to 70 GHz). The measured ON state s_{21} was some dB higher than anticipated which could be explained by somewhat higher switch losses.

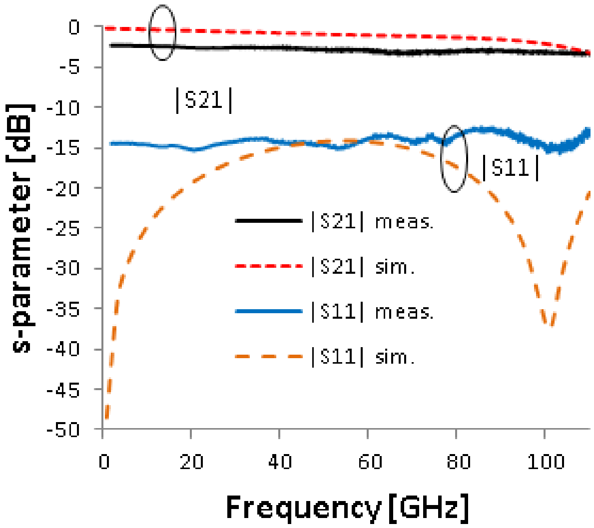

a)

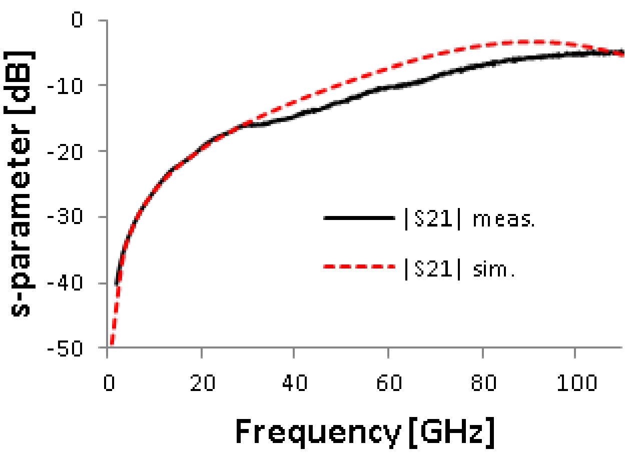

b)

Figure 9. Measured and simulated s-parameters (incl. RF pads) of a CPW RF-MEMS SPST series switch circuit (made on a 200 µm GaAs wafer): a) down-state (ON) s_{21}/s_{11} and b) up-state (OFF) s_{21}.

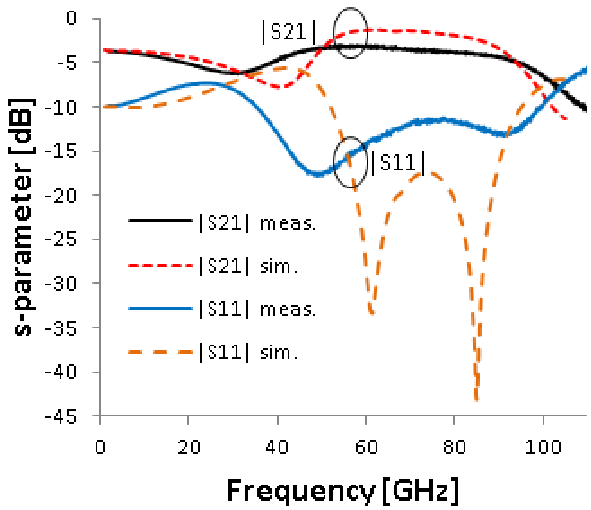

a)

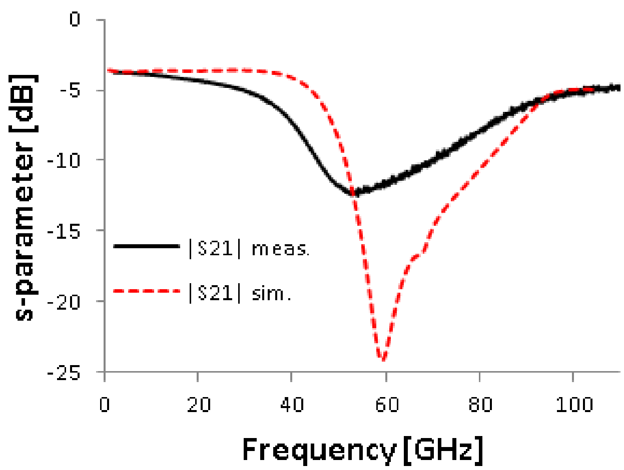

b)

Figure 10. Measured and simulated s-parameters (incl. RF pads) of a V-band CPW RF-MEMS Dicke switch circuit (made on a 200 µm GaAs wafer): a) ON state s_{21}/s_{11} and b) OFF state s_{21}.

Figs. 10a-b show the measured and simulated results (non-deembedded data) of a V-band GaAs MMIC RF-MEMS (Dicke) switch test circuit shown in Fig. 8 (to the right). Compared with the simulations, the experimental (s_{21} and s_{11}) switch data is shifted down somewhat in frequency which may be explained by the switch circuit models used (see Fig. 9). The measured in-band losses and isolation of the V-band Dicke MEMS switch design (that include also the RF pad losses) are slightly higher/lower than anticipated (3 dB/12 dB measured and 1 dB/24 dB simulated at 60 GHz, respectively). The active circuit dimensions of the CPW GaAs RF-MEMS wideband SPST and V-band Dicke switch designs are equal to 650 µm x 520 and 650 µm x 1600µm, respectively.

Fig. 11 shows a photograph of a fabricated W-band on-chip slot antenna that was included on the same GaAs MMIC wafer run. The GaAs slot antenna is fed by a CPW line connected at the center part. The E-field distribution within the slot is at its maximum in the center and diminishing at the edges. The impedance can be chosen depending on the location of the feeding (lowest at the edges). The total length and the width of the slot antenna were taken into consideration for the impedance matching of the antenna to a CPW feed line (with 25 µm line width and 8 µm slot width). The design was made considering a GaAs wafer (ε_r = 12.9) and where the metallization (simulated as a perfect electric conductor) is embedded in between two layers of SiN (ε_r = 6.8). The antenna dimensions were fixed to 1500 µm by 500 µm which imposed the edges of the antenna to be bent. Whatever shapes the antenna takes, it will still radiate if the surface currents travel around the slot perimeter with a perimeter equal to one lambda at the operation frequency.

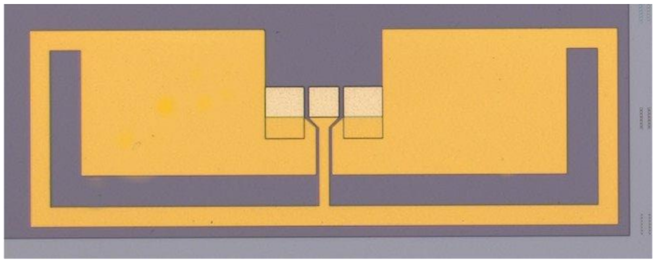

Figure 11. Micrograph of W-band GaAs MMIC on-chip slot antenna.

Measured and simulated s_{11} of the W-band GaAs on-chip slot antenna are shown in Fig. 12. According to simulations the GaAs on-chip antenna is matched between 95-102 GHz ($s_{11} \leq$-10 dB) corresponding to an s_{11} -10 dB bandwidth of 7%. The corresponding measured s_{11} bandwidth is 17% ($s_{11} \leq$-10 dB at 90-107 GHz). The simulated radiation pattern is roughly omnidirectional with a maximum gain of 1 dBi.

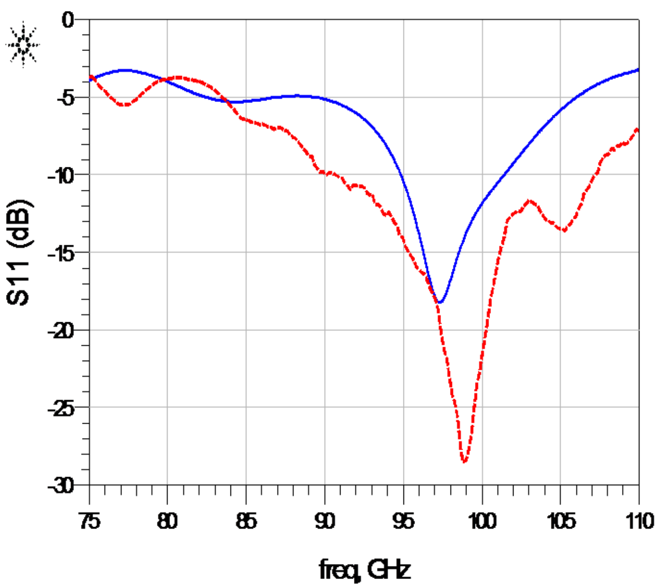

Figure 12. Simulated and measured s_{11} (thin blue and thick red lines, respectively) of a fabricated W-band GaAs MMIC on-chip slot antenna.

CONCLUSIONS

We presented some 0-level packaged GaAs MMIC based low-loss RF-MEMS (series and shunt) switches that potentially may be used in very wideband (e.g. DC-40 GHz) switching and power limiter circuits. A Ka-band GaAs MEMS 3-bit phase shifter (realized within a compact circuit area of 4 mm^2) obtained a minimum in-band loss of 4 dB at 32 GHz. LTCC based packaging (phased array antenna) modules intended for such highly integrated GaAs MEMS mm-wave phase shifting devices were also presented. Finally, we presented a V-band GaAs RF-MEMS Dicke switch network with 3 dB/12 dB of in-band losses/isolation and a wideband (90-107 GHz) GaAs on-chip slot antenna. The reconfigurable broadband GaAs MEMS switch circuits and antennas may be used in highly integrated adaptive front-ends for wireless communication and RF sensing applications up to W-band.

ACKNOWLEDGMENT

The authors wish to acknowledge the European Union for the funding and support of the FP7 ICT projects MEMS-4-MMIC (Grant Agreement no. 224101) and NANOTEC (Grant Agreement no.288531).

REFERENCES.

[1] http://www.radantmems.com

[2] M. Kim, J.B. Hacker, R.E. Mihailovich, J.F. DeNatale, "A monolithic MEMS switched dual-path power amplifier," *IEEE Microwave & Wireless Comp. Lett.*, vol. 11, no. 7, pp. 285-286, July 2001.

[3] J.B. Hacker et al., "Monolithic PHEMT MMICs integrated with RF MEMS switches," *2004 IEEE Compound Semiconductor Integrated Circuits Symp.*, pp 229-232, Oct. 2004.

[4] R. Malmqvist et al., "A K-band single-chip reconfigurable/ multifunctional RF-MEMS switched dual-LNA MMIC," *2012 IEEE MTT-S Int. Microwave Symp. Dig.*, June 2012.

[5] S. Seok et al., "Wafer-level BCB CAP packaging of integrated MEMS switches," *2012 IEEE MTT-S Int. Microwave Symp. Dig.*, June 2012.

[6] A. Persano, A. Tazzoli, A. Cola, P. Siciliano, G. Meneghesso, F. Quaranta, "Reliability enhancement by suitable actuation waveforms for capacitive RF MEMS switches in III-V technology," *IEEE J. of Microelectromechanical Systems*, vol. 21, no. 2, pp. 414-419, April 2012.

[7] R. Malmqvist et al., "Design, packaging and reliability aspects of RFMEMS circuits fabricated using a GaAs MMIC foundry process technology," *2010 European Microwave Integrated Circuits Conference*, Oct. 2010.

[8] J. B. Hacker, R. E Mihailovich, M. Kim, and J. F. DeNatale, " A Ka-Band 3-bit RF MEMS True-Time-Dealy Network," IEEE Trans. Microwave Theory Techniques, Vol. 51, no. 1, Jan. 2003, pp. 305-308.

[9] P. Rantakari et al, "Wide-band radio frequency micro electro-mechanical systems switches and switching networks using a gallium arsenide monolithic microwave-integrated circuits foundry process technology," IET Microwaves, Antennas & Propagation, 2011, Vol. 5, Iss. 8, pp. 948–955.